

Available online at www.sciencedirect.com

jmr&t
Journal of Materials Research and Technology
www.jmrt.com.br



Original Article

Evaluation of carbon diffusion in heat treatment of H13 tool steel under different atmospheric conditions

Maziar Ramezani*, Timotius Pasang, Zhan Chen, Thomas Neitzert, Dominique Au

Department of Mechanical Engineering, Auckland University of Technology, Auckland, New Zealand

ARTICLE INFO

Article history:

Received 2 April 2014
Accepted 23 October 2014
Available online xxx

Keywords:

Carburization
Diffusion
H13 tool steel
Hardening
Heat treatment atmosphere
Nitriding

ABSTRACT

Although the cost of the heat treatment process is only a minor portion of the total production cost, it is arguably the most important and crucial stage on the determination of material quality. In the study of the carbon diffusion in H13 steel during austenitization, a series of heat treatment experiments had been conducted under different atmospheric conditions and length of treatment. Four austenitization atmospheric conditions were studied, i.e., heat treatment without atmospheric control, heat treatment with stainless steel foil wrapping, pack carburization heat treatment and vacuum heat treatment. The results showed that stainless steel foil wrapping could restrict decarburization process, resulting in a constant hardness profile as vacuum heat treatment does. However, the tempering characteristic between these two heat treatment methods is different. Results from the gas nitrided samples showed that the thickness and the hardness of the nitrided layer is independent of the carbon content in H13 steel.

© 2014 Brazilian Metallurgical, Materials and Mining Association. Published by Elsevier Editora Ltda. All rights reserved.

1. Introduction

Heat treatment is a process to alter the metallurgical and mechanical properties for specific purposes that involves heating and cooling of the material. It is known that the hardness obtained from hardening process is greatly influenced by the available carbon content in steel during quenching [1]. The presence of carbon within the steel matrix is largely responsible to the obtainable mechanical properties, which makes the steel material a highly useful commodity of everyday life. It also affects both the minimum hardening

temperature and the maximum achievable hardness [2]. To establish a proper heat treatment atmosphere for steel, there is a need to understand the relationship between the atmosphere composition and the carbon content of steel during the austenization period.

Realistic carbon diffusion model for the carbon profile is important. Carbon can either diffuses out or into the steel matrix depending on the working environment [3]. If decarburization happens, the hardness on the surface of the treated material is going to be lower than expected. However, if carburization was conducted, the treated material would be hardened [4]. Many researches have been conducted related to

* Corresponding author.

E-mail: maziar.ramezani@aut.ac.nz (M. Ramezani).

<http://dx.doi.org/10.1016/j.jmrt.2014.10.014>

2238-7854/© 2014 Brazilian Metallurgical, Materials and Mining Association. Published by Elsevier Editora Ltda. All rights reserved.

the carburization process (e.g., [5–8]); however, understanding of the decarburization during heat treatment is still limited, especially for H13 tool steel. Although Arain [9] investigated the difference between the open atmosphere heat treatment and the vacuum heat treatment, his focus was mainly on H13 toughness behaviour. The kinetic of the carbon diffusion within the H13 tool steel is also not yet clear.

Thus, the main objective of this research is to investigate how the surrounding condition during heat treatment process influences the material hardness profile and to study the carbon diffusion kinetic when the material is subjected to different atmospheric conditions during austenitizing stage. Samples of H13 steel would be subjected to heat treatment process with different duration time and under different atmospheric conditions. Hardness profile of each sample would then be analyzed. It is also of interest to investigate the effectiveness of the gas nitriding process. The carbon diffusion kinetic of H13 steel during heat treatment will also be studied. Carbon diffusion process is modelled based on the Van-Ostrand-Dewey solution, and the carbon activation energy and carbon diffusivity at 1020 °C is determined.

2. Experimental procedures

The four different heat treatment and atmospheric conditions investigated in this study are heat treatment without atmospheric control, heat treatment with stainless steel foil wrapping, pack carburizing heat treatment, and vacuum heat treatment. Further treatment would also be conducted to investigate the effect of carbon content on the efficiency of the nitriding case hardening process. After quenching, the samples were subjected to two tempering processes followed by gas nitriding. Between each process, a sample was collected for analysis. Table 1 summarizes the experimental plan.

The samples used in this study have the size of 7 mm × 10 mm × 60 mm with the initial hardness of ~12HRC. For the heat treatment without atmospheric control, the specimens were heated in a muffle furnace at austenitizing temperature of 1020 °C for the specified time period. The samples were positioned at the centre region of the muffle furnace and were in direct contact with the surrounding atmosphere. For this atmospheric condition, carbon in steel could freely react with the ambient atmosphere. An electrical heated open atmosphere furnace (muffle furnace) was used for all heat treatment processes except vacuum heat treatment process. Data logger with a thermocouple was used to monitor and ensure the right treatment temperature was maintained during the process.

In the heat treatment with stainless steel foil wrapping, the specimens were fully wrapped with a piece of stainless steel foil to reduce the rate of chemical diffusion between the specimen and the furnace atmosphere. This method is commonly used in industry and the suggested wrapping procedures can be found in [10]. For this research, each sample was first wrapped with the long side (the length) double folded, then double folded inwardly from the other two ends (the widths). This experiment setting aimed to minimize the continuous carbon reaction and oxidation between the sample and the ambient atmosphere by the existence of stainless steel



Fig. 1 – (a) Stainless steel foil wrapping and (b) pack carburization.

foil. The stainless steel foil acts as a barrier to restrict the carbon reaction between the specimen and the surroundings. The sample wrapped in stainless steel foil is shown in Fig. 1(a).

In pack carburization heat treatment, a steel box holding a specimen was fully packed with charcoal with case hardening crystal, barium salt, chemical formula of $\text{Ba}(\text{ClO}_3)_2$ and was heated to a temperature of 1020 °C. The specimen is located at the centre of the steel box and is fully covered by barium salt, so each specimen surface is in contact with the same carburized atmosphere condition. A photo of the pack carburization experiment before the sample is covered up with barium salt is given in Fig. 1(b).

The vacuum treatment was conducted in an Abar vacuum furnace at approximate 25 μ and preheated at temperature of 650 °C and 850 °C. Each preheating stage took 1 h. Then it was heated up to 1040 °C and held for either 60, 90 or 120 min, and finally cooled to room temperature in a rate of 30 °C/min. Fig. 2 shows the muffle furnace and the Abar vacuum furnace used for this research.

Once the austenitizing time is reached, the specimen must be rapidly cooled from the austenite state to the room temperature to form martensite. Two different cooling methods were applied with the first three atmospheric conditions, i.e., fan cooling and water quenching. For the fan cooling, the specimens were taken out from the furnace and were cooled in front of a running fan. The specimens were kept rotating so the cooling rate would be even on all surfaces. In the water quenching, the specimens were put into a pool of water, and kept stirring in the water for 2 min. Due to practical difficulties, the vacuum heat treated samples were only cooled in the vacuum furnace with 2 bar of nitrogen gas and the cooling rate of 30 °C/min. After the cooling, the specimen dimensions were measured again to look for the size changes during the process. A small sample with the size

Table 1 – Summary of the experiments.

Heat treatment stage experimental planning												
Treatment condition	Heat treatment without atmospheric control			Heat treatment with stainless steel foil wrapping			Vacuum heat treatment			Pack carburization heat treatment		
Sample size	7 × 10 × 60 (mm ³)			7 × 10 × 60 (mm ³)			7 × 10 × 60 (mm ³)			7 × 10 × 60 (mm ³)		
Pre-heat temperature (°C)	815			815			850			815		
Austinitizing temperature (°C)	1020			1020			1040			1020		
Treatment duration (h)	1	3	5	1	3	5	1	1.5	2	1	3	5
Cooling medium	Fan cooling Water quench			Fan cooling Water quench			Vacuum furnace quenching			Fan cooling Water quench		
	1st Sample collection			1st Sample collection								
	1st Tempering at temperature of 540 °C for 4 h			1st Sample collection								
	2nd Sample collection			2nd Sample collection								
	2nd Tempering at temperature of 595 °C for 4 h			3rd Sample collection								
	3rd Sample collection			1st Gas nitriding at temperature of 530 °C for 6.5 h						No gas nitriding treatment		
	1st Gas nitriding at temperature of 530 °C for 6.5 h			4th Sample collection								
	2nd Gas nitriding at temperature of 530 °C for 6.5 h			5th sample collection								
	3rd Gas nitriding at temperature of 530 °C for 6.5 h			6th Sample collection								
	6th Sample collection											

of 7 mm × 10 mm × 10 mm was then cut from each quenched specimens for hardness test and metallographic analysis.

The remaining part of the specimens would then be subjected to two tempering processes which were held at temperature of 540 °C and 595 °C in a vacuum furnace for 4 h. To investigate the dynamics of the carbon content on the efficiency of case hardening by gas nitriding, the last part of the remaining treated samples were cut into three different pieces and subjected to once, twice or thrice times of nitriding case hardening process. Samples from pack carburization experiment would not be subjected to case hardening process because this is not a usual practice in industry. The

gas nitriding process is conducted at 530 °C under controlled atmosphere for 6.5 h.

3. Modelling of carbon diffusion process

Austenization of H13 steel is always conducted at temperature within 995–1040 °C. At such high processing temperature, carbon may diffuse into or out from the material depending on the atmospheric condition and the processing temperature. This is crucial to material mechanical properties because carbon content has direct relationship with the material strength.



Fig. 2 – Furnaces used for heat treatment hardening experiments: (a) muffle furnace and (b) vacuum furnace.

Decarburization process happens when steel reacts to the oxygen, moist or dry oxygen in the atmosphere when it is heated at 600 °C or above where the driving force is the carbon chemical potential across the material and the atmosphere [11]. The most basic stoichiometric chemical reaction of carburization and decarburization is as follow:



This chemical reaction is reversible, and the chemical equilibrium constant (K) can be defined as [12]:

$$\log K = -\frac{8918}{T} + 9.1148 \quad (2)$$

where, T is the temperature in Kelvin. Knowing the partial pressure of the carbon dioxide and the carbon monoxide, the equilibrium weight percent of carbon on steel at the given processing temperature can be predicted as follow [13]:

$$\text{wt\% C} = \frac{1}{K f_c} \frac{P_{\text{CO}}^2}{P_{\text{CO}_2}} \quad (3)$$

where, P_{CO} and P_{CO_2} are the partial pressure of their subscripts, and f_c is the activity coefficient of carbon. Eq. (3) expresses the equilibrium surface carbon content is governed by the operating temperature since K is a function of temperature and the partial pressure of both the carbon dioxide and the carbon monoxide. f_c for Fe–Cr–C alloy system can be calculated using this equation [13]:

$$\log f_c = \frac{2300}{T} - 2.24 + \left(\frac{179}{T}\right) (\text{wt\% C}) - \left(\frac{102}{T} - 0.033\right) (\text{wt\% Cr}) \quad (4)$$

With Eqs. (2)–(4), the following equation can be established to estimate the heat treating atmosphere for small alloying constituents Fe–Cr–C steel system.

$$\log \frac{P_{\text{CO}}^2}{P_{\text{CO}_2}} = \log(\text{wt\% C}) + \frac{179}{T} (\text{wt\% C}) - \left(\frac{102}{T} - 0.033\right) (\text{wt\% Cr}) - \frac{6618}{T} + 6.875 \quad (5)$$

Eq. (1) shows in carburization (right to left) reaction, the gas carbon monoxide in the atmosphere decomposes on the steel surface into the nascent carbon and carbon dioxide. This results in higher carbon concentration on the surface and a concentration gradient of carbon between the surface and the core of material. Based on the diffusion theory, which will be described afterward, the carbon decomposed on metal surface diffuses inward into the metal core until an equilibrium is reached, while the by-product carbon dioxide further react with the carbonaceous material (if there is any) to generate fresh carbon monoxide.

Decarburization (left to right) is a reverse process of Eq. (1) and operates in opposite order of carburization. Carbon in steel reacts with the oxygen in the air to form the carbon dioxide, which further reacts with the carbon in steel and

forms the carbon monoxide. The formed carbon dioxide and carbon monoxide escape to the ambient atmosphere through the pores and cracks in the scale. Min et al. [14] found the thickness of the oxidation film formed during H13 oxidation increases with the processing time and temperature. This is because the hematite formed over the magnetite layer during the oxidation process reduces due to the low diffusion speed of the metal ion and oxygen in hematite phase.

In either carburization or decarburization, carbon moves from high concentration region into low concentration region. This statement does not mean carbon is only moving in one direction. In reality, carbon travels to any direction simultaneously, but in average, a net diffusion flux of carbon diffuses to lower concentration region from high concentration region. For such diffusion process, Fick's Law can be used:

$$J = -D \frac{\partial C}{\partial x} \quad (6)$$

where, J is the diffusion flux per unit cross-section area per time, D is the diffusion coefficient, and $\partial C/\partial x$ is the concentration gradient. The diffusivity of an element can be determined by the Arrhenius reaction equation:

$$D = D_0 \exp\left(-\frac{E}{RT}\right) \quad (7)$$

where, D is the diffusion coefficient, D_0 is the pre-exponential factor (cm^2/s), E is the activation energy for diffusion (J/mol), $R = 8.314 \text{ J/(mol K)}$ and T is the absolute temperature in Kelvin. Eqs. (6) and (7) show that the diffusion flux is governed by the concentration of the diffusing species at any phase, diffusion temperature and the area perpendicular to the diffusion direction. Carbon diffusivity is relatively lower in tool steel than in other steel because it contains many carbide forming elements (Cr, Mo and V) and the presence of Si also reduces the degree of carbon diffusivity. This results in a comparatively thin concentrated carburized layer. Kucera et al. [15] observed that the diffusion rate increases with increasing temperature, it can also be influenced by chemical composition, and the depth of decarburized layer is increased with time.

It should be noted that the Fick's first law cannot be used for carburization/decarburization modelling, as the diffusion flux is changing with time and the concentration gradient is a function of time. So there is a need for the application of Fick's second law, a second derivative model used to describe the time transient diffusion process. Fick's second law is:

$$\frac{\partial C_x}{\partial t} = -\frac{\partial}{\partial x} \left[-D \frac{\partial C_x}{\partial x} \right] = D \frac{\partial^2 C_x}{\partial x^2} \quad (8)$$

where, C_x is the concentration at distance x from a reference point, and t is the time. The average carbon diffusivity (cm^2/s) for most steel can be approximated by [16]:

$$D_c^y = 0.12 \times \exp\left(\frac{-16000}{T}\right) \quad (9)$$

With the following boundary condition: at $t=0$, surface concentration is equal to the surrounding concentration, and considering the material is infinitely long, the concentration on the other side (away from the surface) is equal to the initial

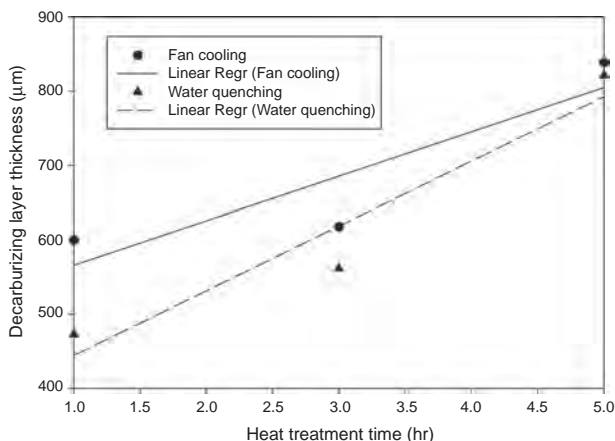


Fig. 3 – Graph of decarburization layer thickness in heat treatment without atmospheric control.

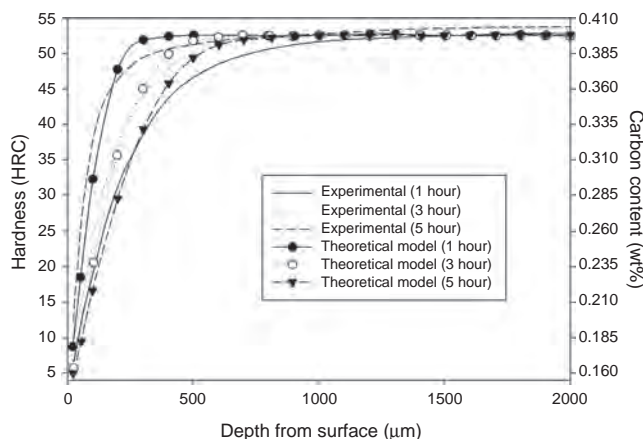


Fig. 4 – Comparison between the experimental value of heat treatment without atmospheric control at 1020 °C followed by fan cooling and theoretical model.

concentration, so Van-Ostrand-Dewey solution to the Fick's second law diffusion equation is defined as follow:

$$\frac{C_x - C_s}{C_0 - C_s} = \text{erf} \left(\frac{X}{2\sqrt{Dt}} \right) \tag{10}$$

The distance measured from the point of drop in carbon content until the point reaching the initial carbon content is termed the total depth of decarburization. However, it is difficult to determine due to the asymptotic manner and is practically insignificant in the industry. Thus, the effective depth of decarburization is used. It is defined as surface distance at ~0.9 of initial carbon content [16].

For this investigation, the carbon content profile is difficult to define without the use of special equipment. Instead, -2HRC of the core hardness was used as a guide to determine the effective decarburization depth. If the average core hardness is 56HRC, the effective decarburization depth would be the point where the hardness reaches 54HRC. This guide was used because ±2HRC is an acceptable value in the heat treatment industry. Through that, the relationship between treatment time and the decarburization layer thickness can be constructed. This is presented in Fig. 3. Two hours of uncontrolled atmosphere heat treatment process gives a decarburization layer thickness of ~0.550 mm. Fig. 3 shows the linearization does not cross the origin of the graph. This is because the rate of decarburization is governed by two simultaneous processes: the surface activity and the diffusion of carbon. Using the Van-Ostrand-Dewey solution (Eq. (10)), the carbon profile can be modelled as:

$$C_x = C_s + \text{erf} \left(\frac{X}{2\sqrt{Dt}} \right) \times (C_0 - C_s) \tag{11}$$

Carbon diffusivity in H13 steel is not yet well published and none of the previous publications were able to provide such a value, so there is a need to determine the carbon diffusivity using the experimental result. In this investigation, the carbon diffusivity is assumed to be independent of carbon

concentration. Thus, by combining Eq. (7) with Eq. (11), it is transformed and gives the following:

$$C_x = C_s + \text{erf} \left(\frac{X}{2\sqrt{[D_0 \exp(-E/RT)]t}} \right) \times (C_0 - C_s) \tag{12}$$

Through the application of the carbon profile equation (Eq. (12)) and setting D_0 as 0.12, the initial carbon content as 0.4, the temperature as 1293K and t as 3600 s, 10,800 s and 18,000 s for 1 h treatment, 3 h treatment and 5 h treatment, respectively, a theoretical carbon content profile at as quenched state after heat treatment without atmosphere control at 1020 °C can be constructed. Through this equation, it was found that the carbon activation energy is 20200J/mol, which gives the carbon diffusivity in H13 steel to be somewhere around $1.97 \times 10^{-8} \text{ cm}^2/\text{s}$ at temperature of 1020 °C by Eq. (7) and the equilibrium surface carbon content is around 0.16 wt%. Fig. 4 shows the comparison between the theoretical loss of the carbon content and the as quenched hardness profile result of those samples heat treated without atmospheric control.

Although Eq. (12) cannot perfectly match the experimental value, it describes the decarburization kinetic reasonably well. By assuming full martensite structure was obtained, a relationship between H13 martensite hardness and carbon content can also be constructed. This shall be a reliable model because through Eqs. (2)–(4), the equilibrium carbon content on the metal surface can be calculated as follow:

$$\log f_c = \frac{2300}{T} - 2.24 + \left(\frac{179}{T} \right) (\text{wt}\%C) - \left(\frac{102}{T} - 0.033 \right) (\text{wt}\%Cr)$$

$$\log f_c = \frac{2300}{1293} - 2.24 + \left(\frac{179}{1293} \right) (0.4) - \left(\frac{102}{1293} - 0.033 \right) (5) = -0.63525$$

$$f_c = 0.23161$$

and,

$$\log K = -\frac{8918}{T} + 9.1148 = -\frac{8918}{1293} + 9.1148, \quad K = 165.3719$$

Also the partial pressure P_{CO} and P_{CO_2} at the operation temperature can be defined using the carburization/

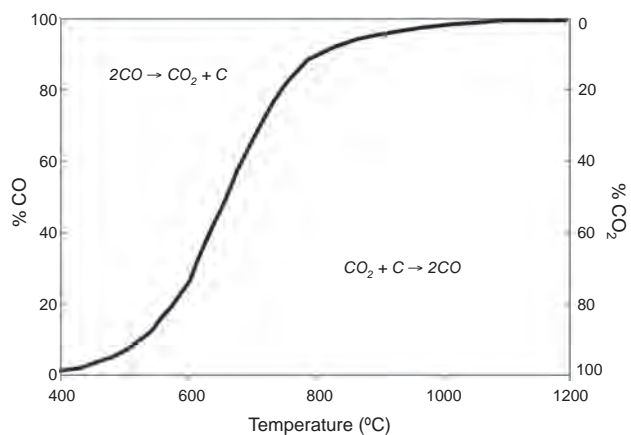


Fig. 5 – Equilibrium diagram for carburization/decarburization reaction at pressure of one atmosphere.

decarburization reaction equilibrium diagram (Fig. 5), where the %CO and % CO₂ at 1020 °C are found to be 98% and 2%, respectively.

The equilibrium weight carbon content on surface can be found using Eq. (3). The chemical equation (Eq. (1)) is used for carburization process, as for decarburization process, it will be transformed into

$$wt\% C = \frac{1}{K_f^2} \frac{P_{CO_2}^2}{P_{CO}} \quad (13)$$

So the equilibrium weight carbon content on surface is:

$$wt\% C = \frac{1}{K_f^2} \frac{P_{CO_2}^2}{P_{CO}} = \frac{1}{(165.3719)(0.23161)} \frac{(101.325 \times 0.02)^2}{(101.325 \times 0.98)} = 0.157$$

This surface weight percent of carbon is in agreement to that shown in Fig. 4. This proves the relationship shown in Fig. 4 between the carbon content and the martensite hardness of H13 steel is valid. Furthermore, by reading the experimental result in Fig. 4 carefully, it was found that the decarburized layer thickness between 1 h hardening and 3 h hardening is wider than the decarburized layer thickness between 3 h treatment and 5 h treatment. It can be explained as the result of the oxide formation of chromium oxide, Cr₂O₃ [17]. The formation of chromium oxide layer acts as a carbon diffusion barrier which slows down the kinetic of carbon diffusion.

4. Results and discussion

Figs. 6 and 7 show the hardness profile for all samples heat treated without atmospheric control and the hardness decrease can be found towards the surface region of all samples. The hardness at the region of 100 μm underneath the surface increases progressively, then the hardness slowly increases towards the constant state. From the figures, it can be seen that there is influence on the material core hardness by the cooling method. The graphs show that samples cooled by water generally have higher hardness (54–57HRC) than samples cooled by fan air (53–54HRC). The

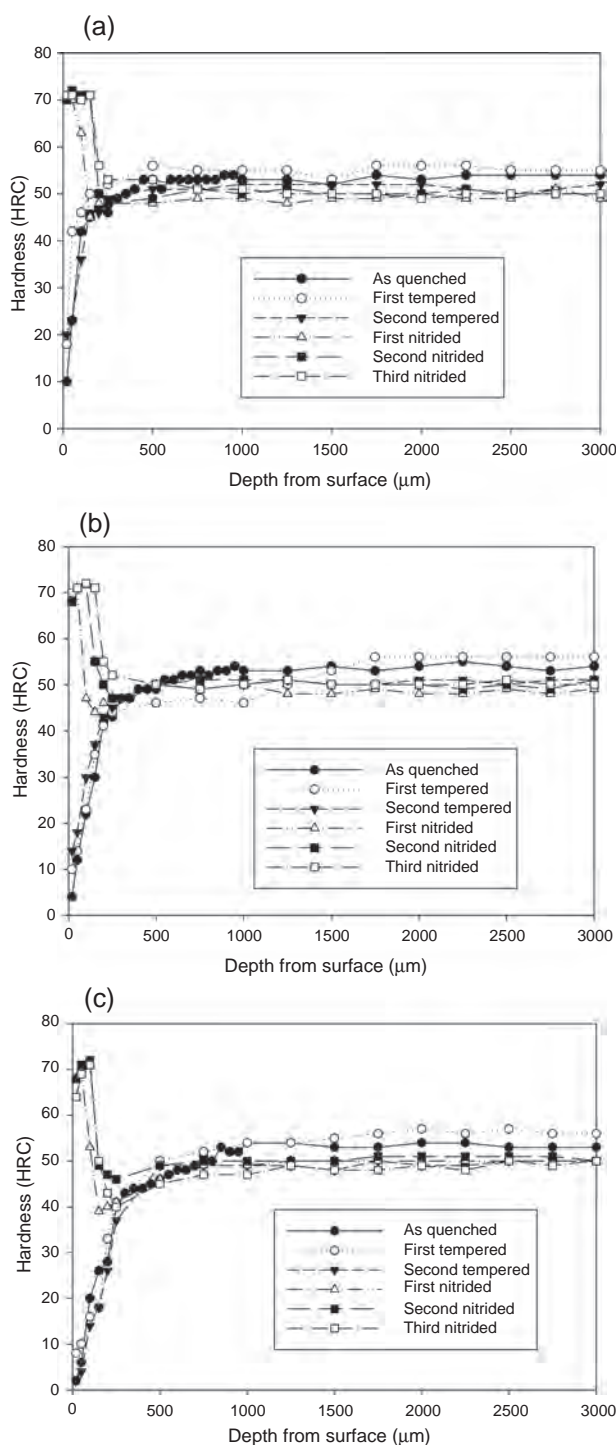


Fig. 6 – Hardness profile of samples heat treated without atmospheric control at 1020 °C followed by the fan cooling and gas nitriding; (a) 1 h heat treatment, (b) 3 h heat treatment, and (c) 5 h heat treatment.

decarburized layer is found to be thicker as treatment time increases. Another notable difference is that the surface hardness (20 μm below the sample surface) of the fan cooled samples are lower than those quenched by water. The fan cooled samples had a surface hardness of 2–10 HRC while the water-quenched samples had a surface hardness of 14–22HRC.

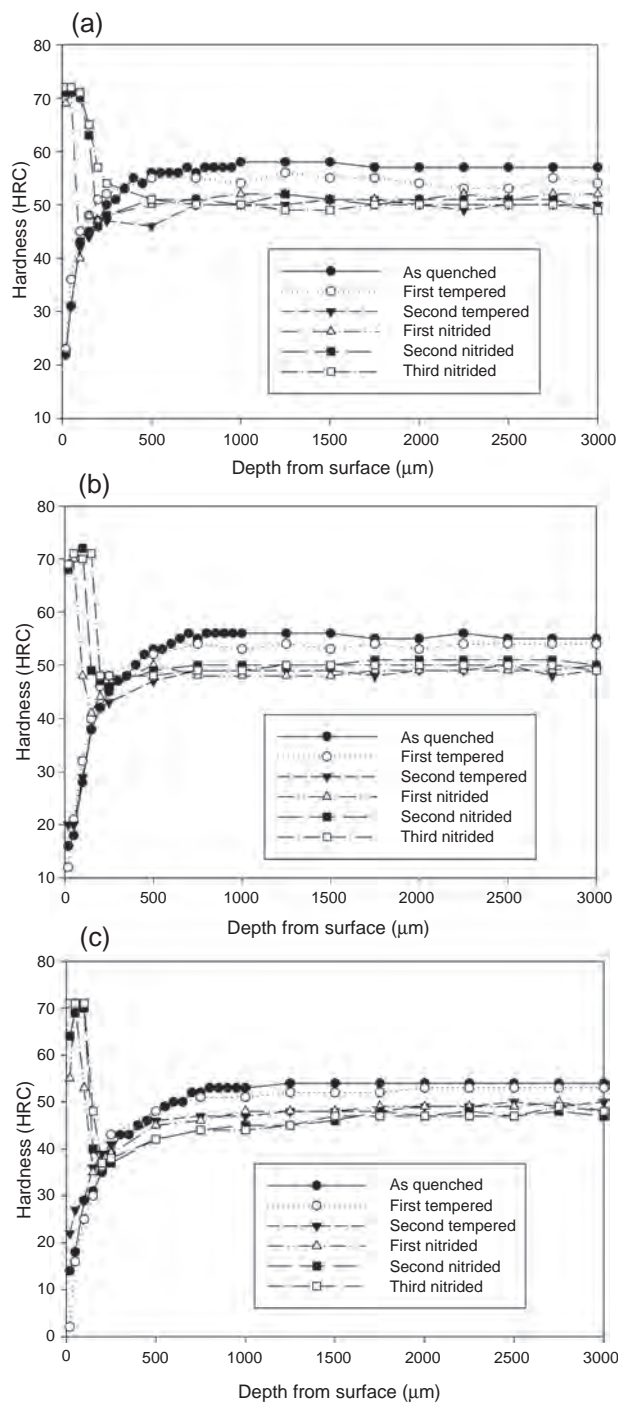


Fig. 7 – Hardness profile of samples heat treated without atmospheric control at 1020 °C followed by the water quenching and gas nitriding; (a) 1 h heat treatment, (b) 3 h heat treatment, and (c) 5 h heat treatment.

The fan cooled specimens had hardness increase after the first tempering stage while water quenched specimens do not show any hardness increase. However, after the second tempering stage, the hardness of both fan cooled samples and water quenched samples dropped to around 46–48HRC. Note that the tempering process does not appear to have any effect on the decarburising zone.

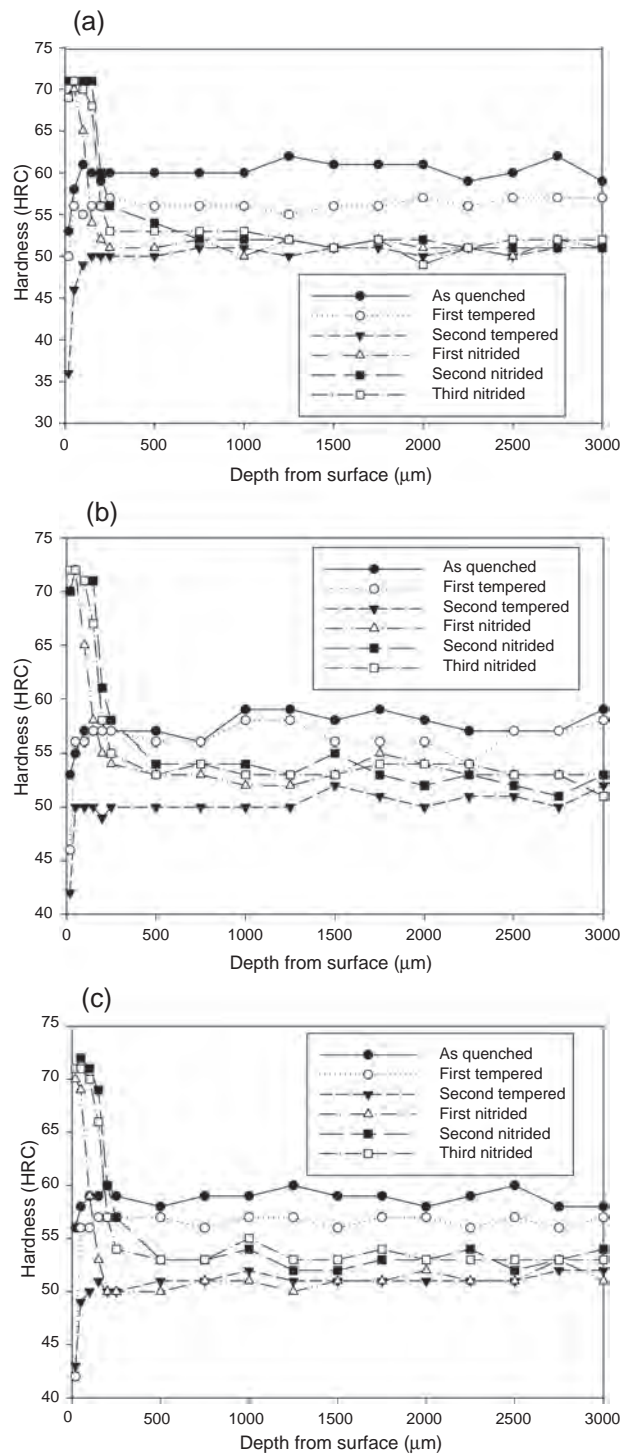


Fig. 8 – Hardness profile of samples heat treated with the stainless steel foil wrapping at 1020 °C followed by the fan cooling and gas nitriding; (a) 1 h heat treatment, (b) 3 h heat treatment, (c) 5 h heat treatment.

The hardness profiles of the samples heat treated with the stainless steel foil wrapping are shown in Figs. 8 and 9. Such heat treatment method results in a reasonably constant hardness profiles throughout the depth of the specimens. The treatment time did not seem to have any direct influence on

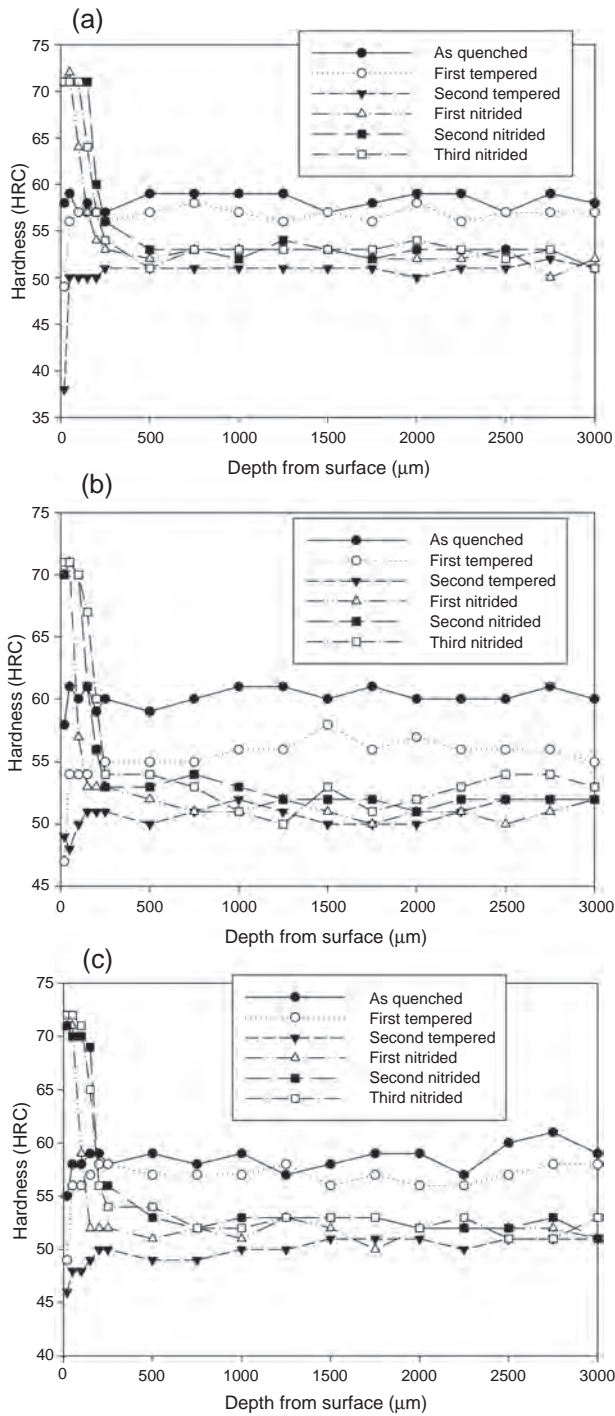


Fig. 9 – Hardness profile of samples heat treated with the stainless steel foil wrapping at 1020 °C followed by the water quenching and gas nitriding; (a) 1 h heat treatment, (b) 3 h heat treatment, and (c) 5 h heat treatment.

the hardness profiles. The results also show that a slight drop in the hardness can be found around 20 μm from the surface. It can be seen that the first tempering process decreases the hardness of the as quenched samples from an average of 59HRC to 57HRC, while the second tempering process further decreases the hardness to around 48–50HRC.

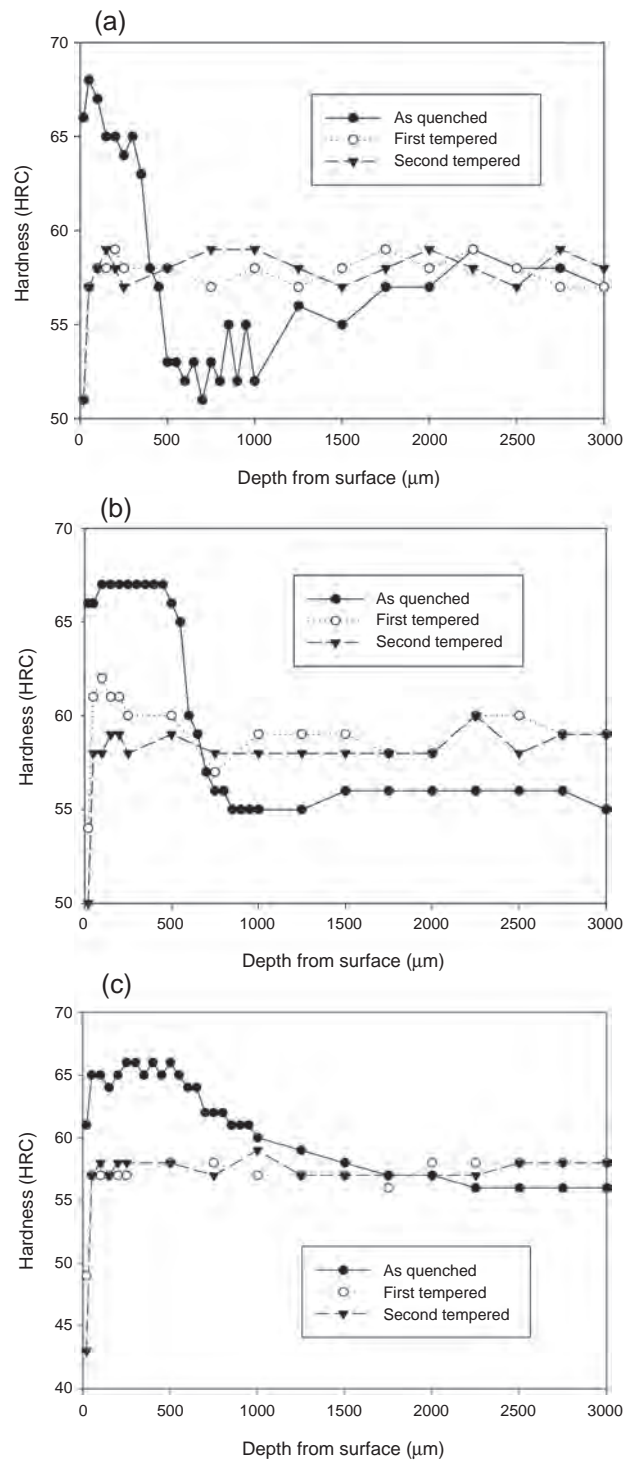


Fig. 10 – Hardness profile of the pack carburized heat treated samples at 1020 °C followed by the fan cooling; (a) 1 h heat treatment, (b) 3 h heat treatment, and (c) 5 h heat treatment.

From the results shown in Figs. 10 and 11, all the samples experienced a hardening effect on the surface after quenching. Beyond the carburized layer, the hardness of all packed carburized samples were approximately the same. It must be noticed that the hardness at the region of 500–1000 μm from

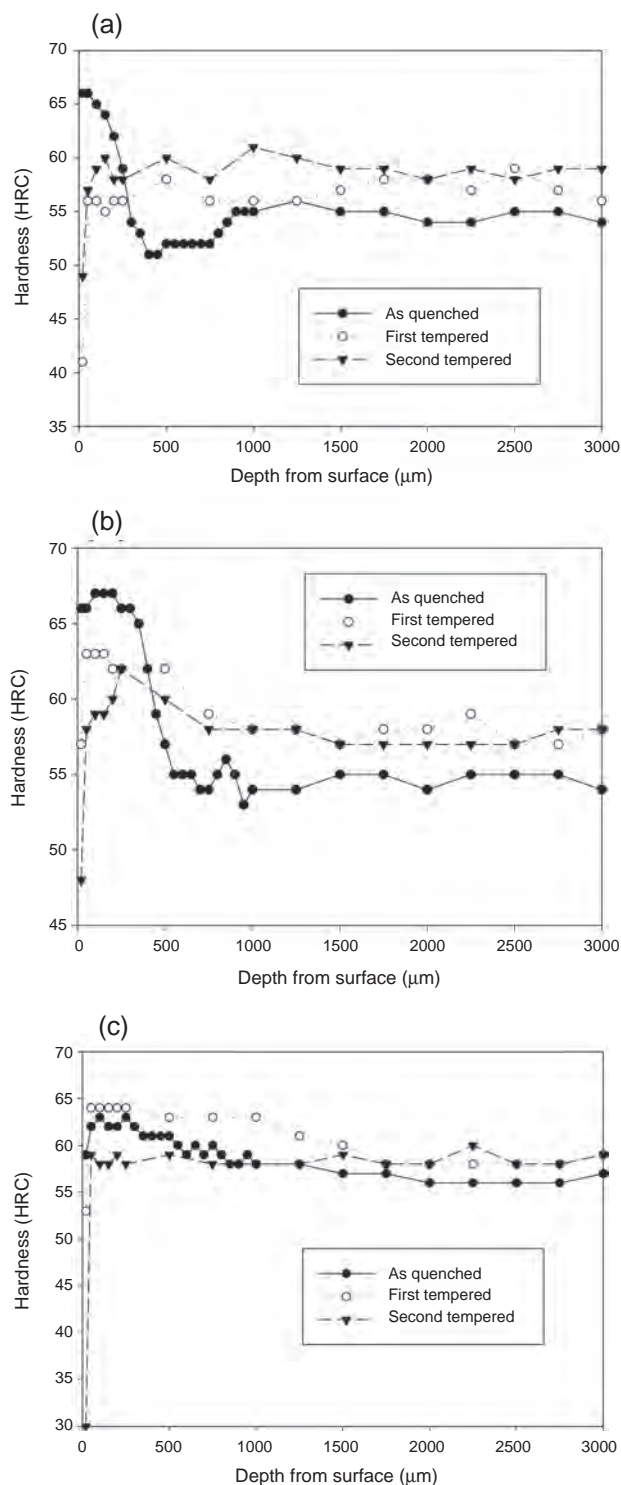


Fig. 11 – Hardness profile of the pack carburized heat treated samples at 1020 °C followed by the water quenching; (a) 1 h heat treatment, (b) 3 h heat treatment, and (c) 5 h heat treatment.

the surface was comparably lower than its core hardness for the sample heat treated for 1 h. This difference does not show in samples heat treated for 3 and 5 h. By studying the hardness profile of the surface region up to 500 μm from the edges, it can be seen that as the treatment time becomes longer, the surface

hardness increases, respectively. The graphs also show that samples cooled by water in fact have lower surface hardness than samples cooled by fan. Hardness increase can be found in the carburized samples cooled by fan after the first tempering stage. The improvement in hardness after the first tempering process is especially significant at the central region of the sample and was increased from 56HRC to 58HRC. The second tempering stage does not show any effect on the hardness. However, if the carburized samples were cooled by water, after the first tempering stage, secondary hardening effect can be found throughout the samples and is especially dominant at the surface region. Great amount of hardness improvement can be found at 1000 μm underneath the surface. After the second tempering process, the hardness profile became constant with the hardness around 59HRC similar to the core hardness of the first tempered condition.

As shown in Fig. 12, there is no indication suggesting the time of heat treatment has significant effect on the hardness of the as quenched samples in vacuum furnace and all as quenched samples have a similar hardness level. No decarburization or carburization layers are found and the hardness varies one or two scale points around 57HRC. It can be seen that if the treatment duration increases the level of hardness variation is lower.

The graphs show that even with a decarburized layer, the nitriding process can still increase the surface hardness significantly up to a certain depth from the surface. Except for the third nitriding process, the first and the second nitriding processes result in hardness improvements after the nitriding process. With increasing heat treatment duration, the surface hardness (20 μm underneath the surface) became lower, respectively. However, the surface hardness was increased with the number of times of the nitriding process. After the nitriding process, the hardness at region 500 μm from the surface increased dramatically. The hardened surface layer becomes thicker as more gas nitriding processes are conducted and the hardness below the hardened layer remains the same level as the hardness of the second tempered condition.

Results have shown that both vacuum heat treatment and heat treatment with stainless steel foil wrapping produce a reasonably constant hardness profile on the as quenched samples. This suggests that the carbon neither diffuses into or out from metal matrix during austenitization. This is reasonable for treatment in vacuum furnace as the carburization cannot be initiated due to the absence of carbon monoxide. For the heat treatment with the stainless steel foil wrapping without continuous supply of the carbon dioxide, it is believed the samples were in decarburization state during austenitization. This can be supported by the drop in hardness at 20 μm underneath the samples surface. However, with the negligible amount of the carbon dioxide inside the wrapping, the decarburization process reaches equilibrium after a short period of time.

Although both the vacuum heat treatment and the foil wrapping heat treatment are able to prevent the decarburization process, they show different tempering characteristics. In the vacuum heat treatment process, secondary hardening can be found after the first temper stage and between the tempering temperature of 500 °C and 550 °C. This secondary hardening effect is the fourth stage of the tempering process.

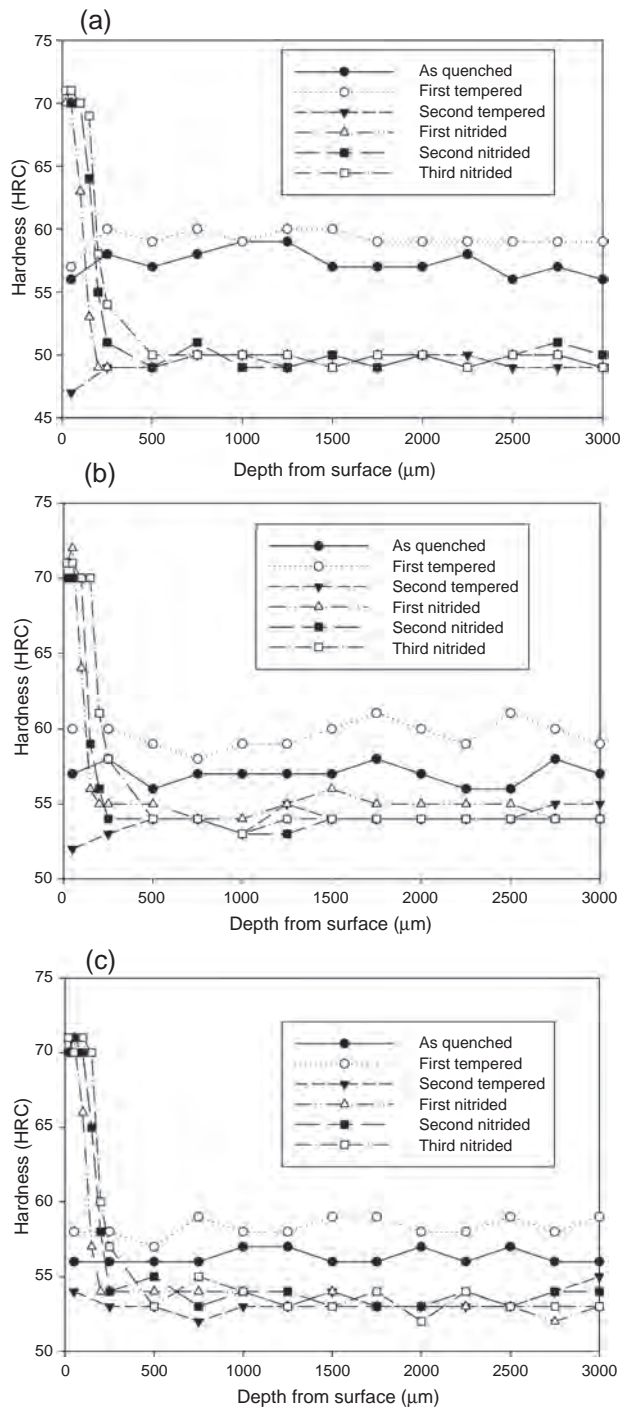


Fig. 12 – Hardness profile of the samples heat treated in the vacuum furnace at 1040 °C followed by the vacuum quenching and gas nitriding; (a) 1 h heat treatment, (b) 3 h heat treatment, and (c) 5 h heat treatment.

From the micrographs shown in Figs. 13 and 14, it can be seen that the samples after the first tempering process are filled with martensite.

For each individual heat treatment method, if the hardness profiles of the nitrided samples are compared with the hardness profile of their second tempered state, the hardness profile beyond the nitrided layer is similar to each other.

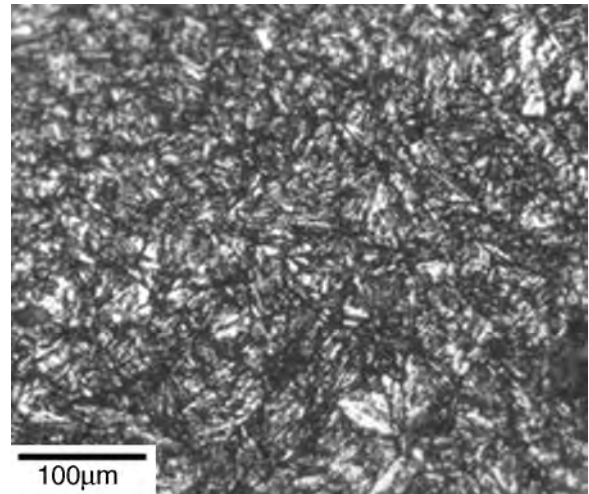


Fig. 13 – Micrograph of the sample after first tempering heat treated in the vacuum furnace.

Through these results, it indicates the gas nitriding process does not alter the microstructure other than within the nitrided region. This can be supported by the micrographs shown in Fig. 15. These micrographs show the comparison between the as quenched state and the nitrided state for the samples heat treated without atmosphere control. The micrographs show the gas nitriding process introduce the harden layer within the decarburized layer by letting nitrogen to diffuse into the core region and alter the surface composition [18], however the compound layer cannot be found on the surface. The results suggest the gas nitriding itself does not have any direct influence on the hardness profile of the inner part of the samples. It is because beyond the nitrided zone, the hardness profile closely matches the hardness profile of the respective second tempered condition. From this, it shows the advantage of using vacuum furnace over the muffle furnace. It is because if the nitrided layer does not cover the decarburizing zone, there is a significant hardness drop below the nitrided

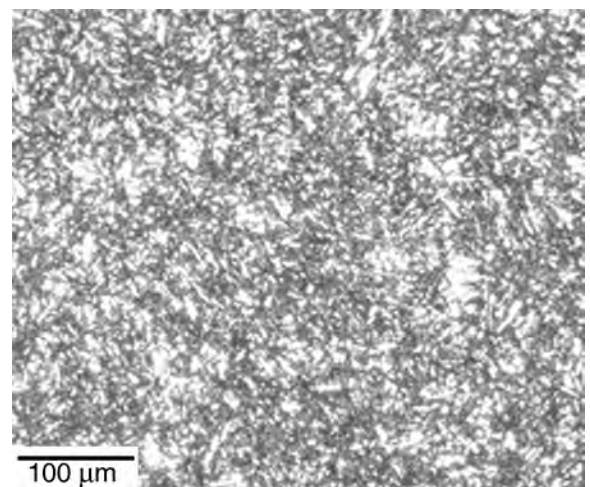


Fig. 14 – Micrograph of the sample after first tempering heat treated in the muffle furnace with the stainless steel foil wrapping.

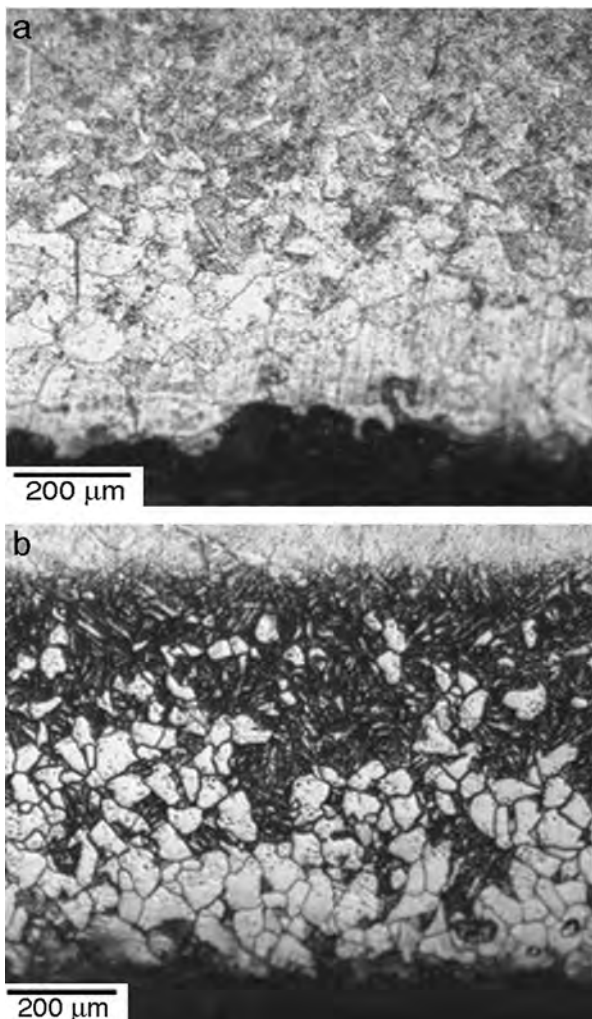


Fig. 15 – Micrograph of the samples heat treated at 1020 °C in an uncontrolled atmosphere for 5 h (a) as quenched state and (b) third nitrided state.

layer, which can result in mechanical failure. This is a realistic case especially for the heat treatment of aluminium extrusion die and is because the recommended thickness of the nitriding layer is not more than ~ 0.3 mm. However the experiments show even 1 h of heat treatment without atmospheric control gives a decarburization layer thickness of ~ 0.5 mm. Thus, there is always a considerable depth of decarburisation layer underneath the nitrided layer. It must also be noted that the thickness of the nitrided layer is not directly proportional to the number of the gas nitriding process being conducted. After second times of gas nitriding process, further case hardening process does not seem to give any hardness improvement.

5. Conclusions

In the study of the carbon diffusion in H13 steel during austenitization, a series of heat treatment experiments had been conducted under different atmospheric conditions and length of treatment. The carbon movement during austenitization of H13 tool steel in the surface region is totally dependent on the

surrounding atmospheric condition. At austenitizing temperature of 1020 °C, without continuous supply of carbon dioxide, carbon molecules in steel tend to react with carbon dioxide in the layer of the iron oxide and escape to the atmosphere. This is the decarburization process and is shown by the heat treatment without atmospheric control experiments. However, the decarburization process can be restricted by either limiting the supply of carbon dioxide, or austenitizing the material in a vacuum environment. With stainless steel foil wrapping, samples were able to maintain their carbon during the heat treatment process and produce a fairly constant hardness profile similar to that of the samples heat treated in vacuum furnace. In the pack carburization experiments, the carbon monoxide was supplied continuously from the surrounding charcoal and caused an increase in the carbon decomposition in the surface and consequently, an increase of hardness. Although each heat treatment condition resulted in a different hardness profile, it did not affect the results for the gas nitriding. All samples subjected to the nitriding process produced similar thicknesses of hardened case layer with average hardness of 70–72HRC.

Conflict of interest

The authors declare no conflicts of interest.

REFERENCES

- [1] Zhang C, Chen R, Luo F, Du C, Shi W. Effect of heat treatment process on microstructure and properties of H13 steel. *Jinshu Rechuli/Heat Treat Metals* 2012;37(10):119–21.
- [2] Tong Q, Wu X-C, Min N. Research on hot-working die steel SDH3 with high hot-strength. *J Iron Steel Res* 2010;22(2):46–50.
- [3] Wang L-P, Wu X-C. Influencing factors of performance for austenitic hot die work steel. *Kang T'ieh/Iron Steel (Peking)* 2008;43(11):78–81.
- [4] Guanghua Y, Xinmin H, Yanqing W, Xingguo Q, Ming Y, Zuoming C, et al. Effects of heat treatment on mechanical properties of H13 steel. *Metal Sci Heat Treat* 2010;52(7/8):393–5.
- [5] Wei Y, Wang G, Sisson RD Jr, Bernard B, Poor R. Intelligent heat treating: simulation of carburization process. In: *ASM heat treating society – 26th conference and exposition: gearing up for success*. 2011. p. 91–8.
- [6] Morizono Y, Tsurekawa S, Yamamuro T. Simplified carburizing process for stainless steel. *Tetsu-To-Hagane/Iron Steel Inst Japan* 2012;98(9):476–81.
- [7] Lin G, Zhang Z, Wang M, Zhu S. Evolution of microstructure and properties of a disk cutter ring material during carburization and heat treatment. *Adv Mater Res* 2013;652–654:1838–41.
- [8] Liu Y, Gao X, Wu Z, Feng X. Influence of high temperature tempering on retained austenite in carburized 20Cr₂Ni₄A steel. *Jinshu Rechuli/Heat Treat Metals* 2013;38(1):77–9.
- [9] Arain A (MSc thesis) Heat treatment and toughness behavior of tool steels (D2 and H13) for cutting blades. Canada: University of Toronto; 1999.
- [10] Bryson WE. Heat treatment, selection, and application of tool steels. 2nd ed. Hanser Publications; 2005. ISBN-13: 978-1569903766.

- [11] Chaus AS, Beznák M. Diffusion in MC carbides in high-speed steels during high-temperature treatments. *Defect Diffus Forum* 2010;297-301:1065-70.
- [12] Harvey FJ. Thermodynamic aspects of gas-metal heat treating reactions. *Metall Trans A* 1978;9(11):1507-13.
- [13] Huang X, Pan J, Shi F, Chen S. Correction model of carbon potential using AI techniques and mechanism analysis. In: 2008 IEEE International conference on cybernetics and intelligent systems. CIS 2008. 2008, art. no. 4670772.
- [14] Min Y-A, Wu X-C, Wang K, Li L, Xu L-P. Prediction and analysis on oxidation of H13 hot work steel. *J Iron Steel Res Int* 2006;13(1):44-9.
- [15] Kučera J, Brož P, Adamaszek K. Decarburization and hardness changes in carbon steels caused by high-temperature surface oxidation in ambient air. *Acta Technica CSAV* 2000;45(1):45-64.
- [16] Verhoeven JD. *Metallurgy of steel for bladesmiths and others who heat treat and forge steel*. USA: Iowa State University; 2005.
- [17] West C, Trindade VB, Krupp U, Christ H-J. Theoretical and experimental study of carburisation and decarburisation of a meta-stable austenitic steel. *Mater Res* 2005;8(4):469-74.
- [18] Akhtar SS, Arif AFM, Yilbas BS. Evaluation of gas nitriding process with in-process variation of nitriding potential for AISI H13 tool steel. *Int J Adv Manuf Technol* 2010;47(5-8):687-98.